Simulating the Effects of Melanin and Air Gap Depth on the Accuracy of Reflectance Pulse Oximeters

Miodrag Bolic [a]

School of Electrical Engineering and Computer Science, University of Ottawa, 800 King Edward Avenue, Ottawa, Canada

Abstract: The work aims to understand the effects of skin color and air gap depth on the accuracy of oxygen saturation estimation. In this paper, this is done by simulating light propagation through the tissue. It is very important to understand light propagation through the tissue when designing a reflectance pulse oximeter to know what tissue layers are illuminated by the LEDs, how to position the emitter and the detector depending on the measurement site, and what kind of signal is expected at the photodetector. This knowledge could also contribute to developing robust pulse oximeters whose accuracy does not depend on a subject's skin color. Our simulation results confirm a larger variation of SpO_2 for lower saturation levels for dark-skinned subjects if the SpO_2 calibration curve is mainly obtained based on measurements from light-skinned subjects. Also, if the device is calibrated with a small air gap, increasing the air gap will result in overestimated SpO_2.

1 INTRODUCTION

The major difficulty when using pulse oximeter devices is motion artifacts. Besides motion artifacts, pulse oximeters are inaccurate in poorly oxygenated patients (Webster, 1997). This is because there is a lack of data for fitting the parameters of the models used in pulse oximeters for patients whose oxygen saturation levels are below 70%. A similar lack of data for calibrating the SpO_2 curve has been noticed for darker-skinned individuals, which might suggest the existence of racial bias. There has been significant interest in racial bias in pulse oximetry. A recent review analyzed the influence of skin pigmentation on the accuracy of pulse oximeters (Fuentes-Guajardo, 2022). It was pointed out that there is growing evidence that pulse oximeters are less accurate in dark-skinned individuals at oxygen saturation levels lower than 80%, resulting in overestimations of the oxygen saturation.

Development of tools for simulating light propagation through non-homogeneous tissues based on Monte-Carlo methods allowed for computational approaches in analyzing the effects of different parameters and skin properties on the distribution of light in the tissue. One of the first works analyzing light propagation through homogeneous and non-homogeneous tissue is (Tuchin, 1997). More recent works include (Reuss, 2004), (Reuss, 2005) and (Chatterjee, 2017).

In this paper, we address issues of estimating oxygen saturation levels in reflectance pulse oximeters for people of different skin colors and, in the case of the different distances between the probe and the tissue, using a model-based design. We simulate light propagation through the tissue using Monte Carlo simulation-based library called MCMatlab (Marti, 2018).

The pulse oximeter probe contains LEDs and a photodetector placed on the same side of the tissue so that the pulse oximeter operates in the reflectance mode. LEDs with 660 nm and 940 nm wavelengths were used. Six layers of skin with different optical properties were simulated. In addition, we added an air gap between the skin and the simulated probe. The light from the LED gets scattered through the tissues, and the photodetector collects only a small percentage of it. We simulated different blood volumes during the systolic and diastolic instants of the cardiac cycle, as well as different oxygen saturation levels of blood. All these parameters affect the percentage of light collected by the photodetector. After obtaining the

[a] https://orcid.org/0000-0002-8013-8645

fraction of illuminated light from the photodetector for the light at 660 nm and 940 nm, we computed the ratio of the fractions of illuminated light (called the ratio of ratios) and used it to estimate the oxygen saturation SpO_2 (Bolic, 2023).

We were especially interested in:
- Analyzing the effects of different levels of melanin on estimated SpO_2,
- Analyzing the effect of changing the air gap depth on estimated SpO_2.

The analysis showed the following results:
- For a given setup, the slope of estimated SpO_2 vs. the ratio of ratios curve differs for different melanin levels. This might explain why there is a bias in estimating oxygen saturation in darker skin individuals.
- Changing the air gap causes large changes in the ratio of ratios which then results in inaccurate SpO_2 estimates.

Besides the Introduction, the paper contains four additional sections. Section 2 provides an overview of the state-of-the-art. Section 3 describes the simulation setup. Section 4 presents the results. Finally, the discussion of the results, conclusion, and future directions are presented in Section 5.

2 BACKGROUND

In this section, we will review the state-of-the-art from several points of view, including racial bias in pulse oximetry, simulation of light propagation through the tissue, and simulation of the effects of skin pigmentation and motion artifacts on pulse oximetry.

The existence of melanin in the skin significantly increases the absorption of light and reduces the fraction of illuminated light received at the detector. The absorbance of 660 nm light by melanin is hundreds of times greater than the absorbance of light at the same wavelength by blood- and melanin-free tissues.

Evaluating the accuracy of existing pulse oximeters for darker skin patients was mainly performed by comparing the pulse oxygen saturation against the reference SaO_2 measurements. The experiments were done on subjects whose oxygen saturation levels were controlled. The results are mixed, but several studies showed an overestimated SpO_2 at lower saturation levels (Bickler, 2005) for darker skin patients.

Light propagation simulators have been developed, including MCMatlab (Marti, 2018), and

used to simulate the effect of melanin on SpO_2 accuracy. Monte Carlo simulations were performed to simulate a transmittance-based pulse oximeter (Arefin, 2022) for different skin color subjects. Virtual patients' finger tissues were generated by modifying the parameters of the tissue. Oxygen saturation was in the range of 70% to 100% for each simulated patient (Arefin, 2022). Monte Carlo light-tissue interaction model that investigated changes in melanin level was proposed for reflectance pulse oximetry (Al-Halawani, 2022). The results show only the photon penetration depth and absorbance and not the effect of melanin on the ratio of ratios and SpO_2 estimation.

It is important to control the pressure when attaching the reflectance probe to the skin. It was shown that over the range of pressure applied to the pulse oximetry probe, the DC amplitude and the normalized pulse area changed significantly (Teng, 2004).

Motion artifacts can be caused even by small movements, such as typing if the probe is placed on the wrist, or breathing if the probe is placed on the shoulder. Motion artifacts can corrupt the signal in different ways. They can cause baseline shift and/or induce changes in the morphology of the signal. Motion artifacts result mainly from the changes in the depth of the air gap between the probe and the tissue with motion. The changes in depth cause changes in the amount of light absorbed in the tissue as well as the amount of light scattered and reflected from the tissue. Motion artifacts are mainly low-frequency interference. The work that included air gap changes in the Monte Carlo model assumed three types of motion: fast arm swing, slow arm swing and typing (Zhou, 2020). The sensor was used in reflectance mode and was placed on the wrist. Recently, several works have been done on characterizing the type of noise or motion artifacts of photoplethysmogram (PPG) signals obtained when people perform different activities such as sitting, walking and running (Cajas, 2020).

3 THE MODEL AND SIMULATION SETUP

3.1 Simulating Light Propagation Through the Tissue

The first step in simulating light propagation through the tissue is to describe the experiment, which includes the modeled tissue and its properties, the

light source and the detector. In the next step, the light is simulated as photons that are absorbed or randomly scattered as they travel through the medium. The rate of absorption and scattering depends on the absorption and scattering coefficients of each layer of the skin. This light distribution is described by the solution to the radiative transfer equation, which is solved using Monte Carlo (MC) methods (Wilson, 1983).

Using tools such as MCMatlab, the implementation of the radiative transfer equation solver is provided so that the user only needs to describe the experiment and interpret the simulation results. MCMatlab is an open-source Matlab-based software for modeling light interaction with biological tissue. MCMatlab includes the radiative transfer equation solver for finding the light distribution in complex media and a thermal solver, which was not used here. It is user-friendly and contains many examples that can be modified and adjusted to a particular problem. However, even though the authors claim significant improvements in computational time compared with other tools (Marti, 2018), MCMatlab is based on Monte Carlo simulations and takes significant time to complete a simulation.

The simulation is mainly based on the work described in (Reuss, 2004) and (Reuss, 2005). The simplified model of a reflectance PPG probe consists of an emitter and a detector. The wavelengths of 660 nm and 940 nm were used in the simulation. Emitter and detector separation was set to 3 mm. The emitter (LED) is centered at the coordinates (-0.15 cm, 0 cm, 0 cm) while the detector is placed at (0.15 cm, 0 cm, 0 cm) and normal to the tissue surface – see Figure 1a). On the emitter side, a Gaussian beam of a radial width of 4 mm was simulated. The Gaussian beam was selected because it approximates noncollimated LED (the light does not have parallel rays). The detector was simulated with a diameter of 2 mm.

Tissue is modeled using several layers and presented as a cuboid in a 3D Cartesian coordinate system. The thicknesses and blood volume distributions in the tissue layers are adapted from (Reuss, 2005). Human skin is divided into epidermis, dermis and hypodermis (Figure 1a)). The optical barrier between the LED and the photodetector is also modeled and shown in red in Figure 1a). The blue color layer around the barrier represents the air gap.

Figure 1b) shows the normalized fluence rate of the collected light at the photodetector. This example is simulated for 660 nm wavelength, with 10 min simulation duration, which allows for simulating

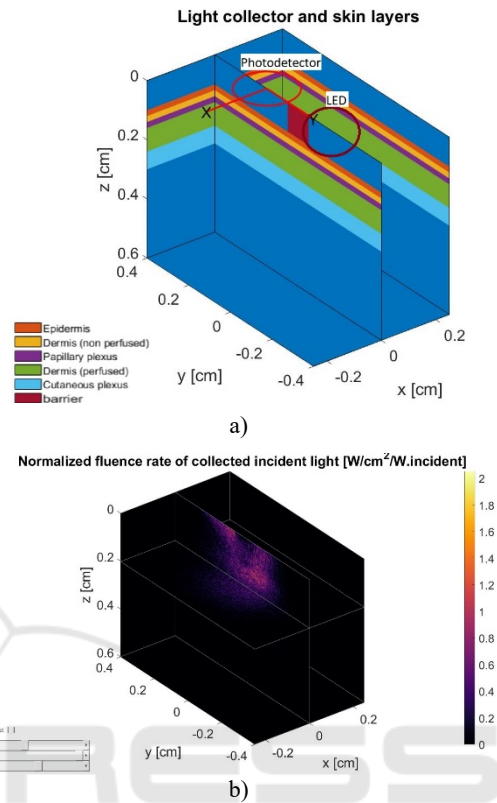about 10^7 photons. We can see a non-uniform distribution of light.

Figure 1: a) Modeled skin layers and b) normalized fluence rate of the collected light. The figure is obtained by running a modified example provided by MCMatlab (Marti, 2018).

3.2 Modeling Changes in Blood Volume

Table 1: Sublayers of the skin together with their thickness and diastolic blood volume.

Layer # (i)	Layer names	Sublayer Thickness (mm)	Blood volume (%)
1	Epidermis	0.2	0
2	Dermis	0.2	0
3	Papillary plexus	0.2	0.0556
4	Dermis (perfused)	0.8	0.0417
5	Cutaneous plexus	0.6	0.2037 in diastole, 0.2454 in systole
6	Hypoderm.	8	0.0417

Since each layer is uniformly thick and has the same area, their relative volumes are expressed only by their thicknesses. Modeled thickness d_i of skin layer

i and the relative volume of blood B_i in each layer are presented in Table 1.

The total blood fraction B_0 is defined as the mean concentration of blood in the total tissue volume during the diastolic stage, and it is assumed to be 5%. Therefore, the values of the diastolic blood volume and the depth of the tissue are selected in a way that the total blood fraction ends up being 5% by computing the total blood fraction as:

$$B_0 = (\sum_{i=1}^{6} d_i B_i)/d_0 \qquad (1)$$

where $d_0 = \sum_{i=1}^{6} d_i$.

Software packages for simulating light propagation through the tissue do not automatically include information about the parameters that change over time. Therefore, modifications must be done to address variables that change over time, such as arterial blood volume. The systole was simulated by increasing blood volume only in the skin layer that contains larger blood vessels. The increase in blood volume per different sublayers was based on the work of Reuss (2005). The arterial pulsation was simulated by blood volume increase in the cutaneous plexus layer only by adding the arterial blood. The pulse fraction B_p is defined as the fraction of the total volume displaced by the arterial pulse, which is assumed to be 0.25%. The relative volume of systole in the cutaneous plexus layer is then computed as $B_5' = B_5 + B_p d_0/d_5 = 0.2037 + 0.0025 \cdot 10mm/ 0.6mm = 0.2454\%$. In this way, the relative volume of blood in the cutaneous plexus changed from $B_5 = 0.2037\%$ to $B_5' = 0.2454\%$. In all other layers, the relative volume of blood is the same during systole and diastole.

In this simulation, about 84% of incident light hits the cuboid boundaries, and 16% is absorbed within the cuboid. Out of the total incident light hitting the boundaries of the cuboid, about less than 1% is detected by the detector placed on the skin's surface. Selected simulation parameters for dermis layers include the water content $W = 0.65$, Mie scattering coefficient 1.0, and anisotropy $g=0.9$.

3.3 Modeling the Level of Melanin

The level of melanin is initially set to 0.3% (Chatterjee, 2017), which is ten-fold below what is commonly found in lightly-pigmented human skin. The reason was to collect a larger illumination fraction than the one collected for the skin with larger levels of melanin. The other melanin levels that are simulated are 3%, 8%, 12% and 16%. The barrier and the airgap depths were kept close to zero, which simulated the situation without the air gap.

The experiment is set to take 20 minutes to obtain one data point on the graph in Figures 2-3. In Figure 2, there are 44 data points resulting in an 8-hour long simulation. These experiments were done for mentioned five levels of melanin. Ideally, the experiment should run for more than 20 minutes per point and be repeated multiple times to reduce the results' variability. The reason for variability is that the photodetector actually collects a very small percentage of light, and if the experiment is short, the illumination fraction will vary a lot.

3.4 Modeling Changes in Air Gap Depth

The effect of different amounts of pressure applied to the probe is simulated by changing the depth of the air gap. Simulation is performed starting with the air gap of 0.05 mm, which corresponds to the situation without the air gap, to 0.2 mm, which corresponds to a small air gap for a smartwatch. The barrier between the LED and the photodetector is simulated as well. Without the barrier, the majority of light collected by the photodetector would be reflected from the skin surface. Motion artifacts are commonly simulated as changes in the air gap depth; therefore, this simulation could be further extended to the simulation of motion artifacts. The melanin level was set to 0.3%.

4 RESULTS

4.1 Oxygen Saturation vs. the Level of Melanin

Figure 2 was obtained by simulating the interaction of light with the tissue for the experimental setup described previously when oxygen saturation was set to 60%, 70%, 80%, 90%, 95% and 100%. The blood volume was changed in the cutaneous plexus layer to simulate the increase of blood volume during the systole. Therefore, there are two different curves for each wavelength, one obtained during systole and another obtained during the diastole period of the cardiac cycle. Figure 2a) shows the relative values of the illumination fraction $I_{dia}^{(660nm)}$, $I_{dia}^{(940nm)}$, $I_{sys}^{(660nm)}$, and $I_{sys}^{(940nm)}$ vs. SpO_2 for a melanin level of 3% that corresponds to lighter skin color. $I_{dia}^{(\lambda)}$ and $I_{sys}^{(\lambda)}$ are the relative intensity of light for a particular wavelength (red 660 nm and infrared 940 nm) detected during systole or diastole.

Figure 2b) shows the relative values of $I_{dia}^{(660nm)}$, $I_{dia}^{(940nm)}$, $I_{sys}^{(660nm)}$, and $I_{sys}^{(940nm)}$ vs. SpO₂ for a melanin level of 12% that corresponds to darker skin color. The illumination fractions are reduced when the melanin level is increased because more light gets absorbed with increased melanin levels.
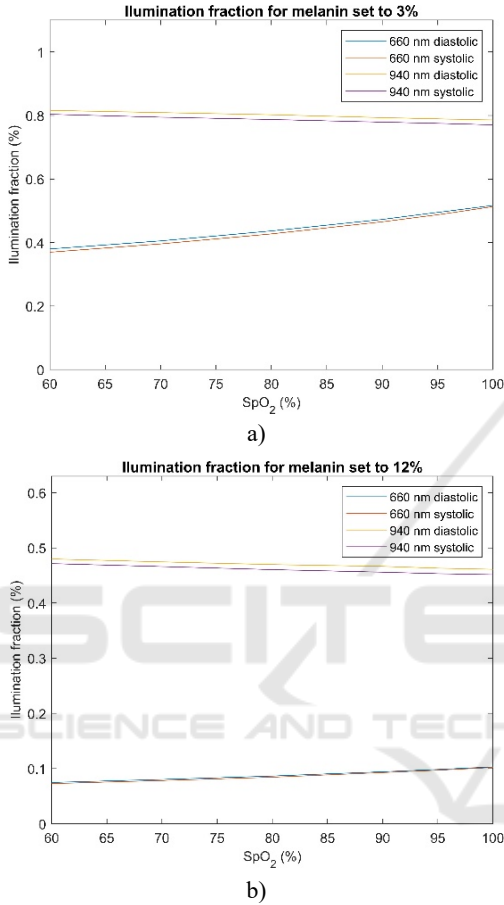

a)

b)

Figure 2: Illumination fractions of light versus oxygen saturation levels obtained at the detector for 660 nm and 940 nm wavelengths for the melanin levels of a) 3% and b) 12%.

Figure 3 shows the illumination franctions for the case when melanin levels take values of 0.3%, 3%, 8%, 12% and 16% for oxygen saturation of 95%. The illumination fractions for both wavelengths are reduced when the melanin level is increased.

The ratio of ratios R is computed as

$$R = \frac{\dfrac{I_{dia}^{(660nm)} - I_{sys}^{(660nm)}}{I_{dia}^{(660nm)}}}{\dfrac{I_{dia}^{(940nm)} - I_{sys}^{(940nm)}}{I_{dia}^{(940nm)}}}$$

We use the illumination fraction instead of the light intensity to compute R. After R is computed, SpO_2 is estimated using regression. An example of linear regression is shown below:

$$SpO_2 = C_A + C_B \cdot R$$

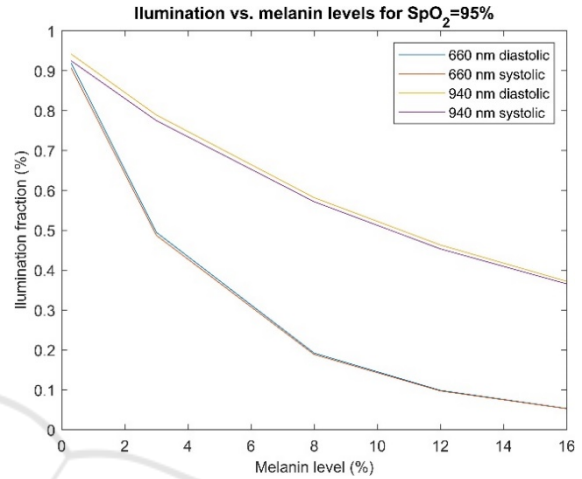where C_A and C_B are regression coefficients.

Figure 3: Illumination fraction of light versus the level of melanin for 95% oxygen saturation level obtained at the detector for 660 nm and 940 nm wavelengths.

For each ratio of ratios obtained using different levels of melanin, we fit different curves. Fitted curves of SpO₂ versus the ratio of ratios for each level of melanin, are shown in Figure 4. The fitted curve for a melanin level of 8% (yellow line) is an outlier.
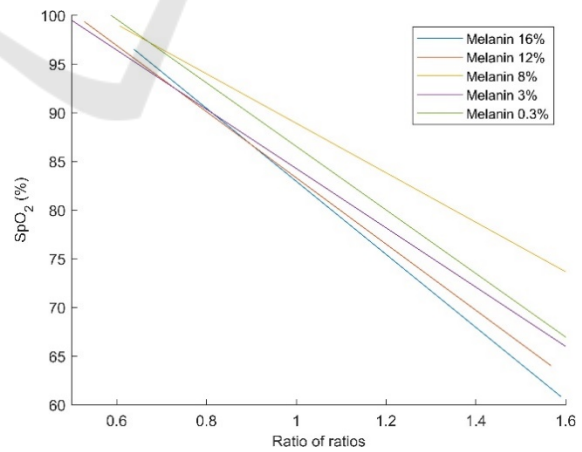

Figure 4: SpO₂ versus the ratio of ratios computed for different melanin levels.

Next, let us consider the following scenario. The simulated data was collected for the case of a low level of melanin (3%), and the regression curve SpO₂

vs. the ratio of ratios was fitted for this melanin level. Then, new simulated data (illumination fraction at 660 nm and 940 nm at systolic and diastolic instances) was collected for subjects with other melanin levels.
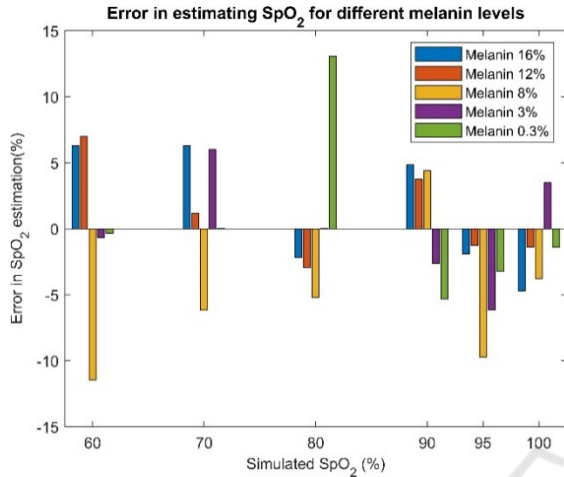

Figure 5: Error in estimated SpO_2 versus simulated (ground truth) SpO_2 computed for different melanin levels.

To compute the SpO_2 for these subjects, the regression coefficients computed for the subject with 3% melanin were used. The error between the computed oxygen saturation levels versus true, simulated oxygen saturation when melanin levels take values of 0.3%, 3%, 8%, 12% and 16% are shown in Figure 5. The abscissa is the simulated SpO_2 at the saturation levels of 60%, 70%, 80%, 90%, 95% and 100%. The ordinate shows the SpO_2 errors for these simulated levels of oxygen saturation. There are several outliers in the figure, including a large outlier at SpO_2=80% for a melanin level of 0.3%. The number of outliers could have been reduced if the simulation time was longer.

4.2 Oxygen Saturation Changes with Air Gap Depth Changes

Figure 6 shows the change of the illumination fraction for both red and infrared light at the points of minimum and maximum blood volume (diastolic and systolic points) for an oxygen saturation level of 95% and a very low level of melanin. The ratio of AC and DC components decreases with the increase of the air gap.

The ratio of ratios is computed from Figure 6 and used to estimate SpO_2, which is shown in Figure 7. Since the SpO_2 is fitted using a curve based on almost no air gap, we see that the SpO_2 gets overestimated as the depth of the air gap increases. The simulation was performed with SpO_2=95%. As can be seen in Figure
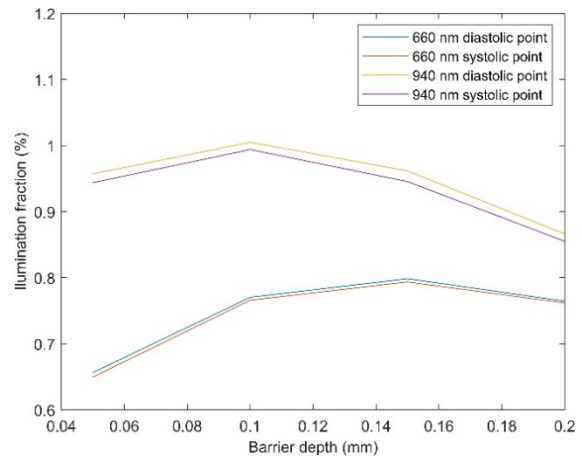

Figure 6: Simulated changes in the illumination fraction with an increased air gap between the probe and the tissue for SpO_2=95%.

7, for larger values of the air gap, we are getting oxygen saturation levels of more than 100%, which is not possible. In a realistic device, an algorithm would limit the SpO_2 level to a maximum of 100%. Devices are normally calibrated for a fixed air gap depth. However, when the air gap depth changes due to motion artifacts, it causes significant changes in the ratio of ratios and errors in estimating SpO_2.
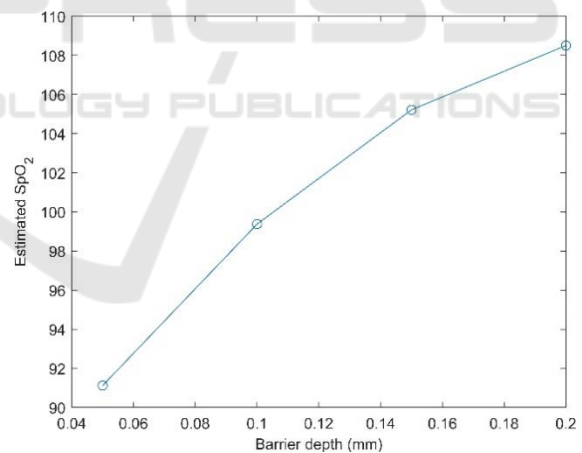

Figure 7: Estimated SpO_2 for the air gap depth of 0.05 mm, 0.1 mm, 0.15 mm and 0.2 mm with a simulated barrier placed between the emitter and the detector for SpO_2=95%. The estimated values of SpO_2 for larger air gaps are outside the bounds (larger than 100%).

5 DISCUSSION AND CONCLUSIONS

This work builds on the modeling works of (Reuss, 2005) and the simulator design of (Marti, 2018). It

analyzes the effects of melanin and the depth of the air gap on the ratio of ratios and the accuracy of SpO_2 estimates. The main observations from this work and future directions are discussed next.

It can be observed from Figure 4 that the slopes of SpO_2 vs. the ratio of ratios curves are different for different skin colors. Therefore, if we could estimate the tone of the subject's skin, we would be able to adjust the curves or select the appropriate regression curve for calibration. In addition, if the SpO_2 calibration curve computed for subjects with a lower level of melanin is used for subjects with a larger level of melanin, the results from Figure 5 do not confirm that the overestimation would occur. This might be because of outliers of SpO_2 estimates at 0.3% and 8% melanin levels. The results, however, show variability with an increased level of melanin.

The illumination is significantly reduced with the increased level of melanin, as shown in Figure 3. It drops faster for red than for infrared light. This information can be used to increase the radiated power of the LEDs in case a darker skin color is detected.

In reflectance pulse oximetry, it is difficult and sometimes impossible to control how well the probe is attached to the skin. This can result in a varying air gap. Increasing the air gap results in an increased level of reflection of light from the surface of the skin, resulting in less light propagating in the tissue and a weaker AC component of the signal. Figure 6 shows changes in illumination fraction at the photodetector with increasing the air gap and barrier depth. Figure 7 shows changes in the estimated SpO_2 for the same case. Therefore, the pressure applied to the device should be controlled and constant to allow for a fixed air gap. Also, motion artifacts cause varying air gaps; therefore, they should be detected, and the signal obtained during motion artifacts should be removed from the analysis.

The study can be extended in several ways. One is to repeat measurements for different points and to run Monte Carlo simulations longer to get less noisy data. We can also modify the tissue model to more precisely reflect the body site where the probe is attached. For example, the optical properties and thickness of the skin layers on the finger, ear, wrist, neck, or forehead (which are some of the typical sites) are different.

The simulated depth of the blood vessels can be modified based on the selected site. In the simulation, we assume that the blood volume changes occur only in the cutaneous plexus. It was also observed (Mannheimer, 2004) that placing the reflectance pulse oximetry probe directly over a larger blood vessel can degrade SpO_2 estimation accuracy. This can also be modeled.

Future work will also include building an end-to-end pulse oximeter simulator that will include the model of the LEDs and driving circuits, the model of the tissue and light propagation and the model of the photodiode and the front-end electronics. This will allow us to understand further how noisy the signal is in case of small levels of illumination of the photodetector and to perform sensitivity analysis to understand what components/parameters of the system affect the output the most.

REFERENCES

Al-Halawani, R., Chatterjee, S. & Kyriacou P.A. (2022). Monte Carlo Simulation of the Effect of Human Skin Melanin in Light-Tissue Interactions. *2022 44th Annual International Conference of the IEEE Engineering in Medicine & Biology Society (EMBC)*.

Arefin, M.S., Dumont, A.P. & Patil, C.A.(2022). Monte Carlo based simulations of racial bias in pulse oximetry. *Proc. SPIE 11951,Design and Quality for Biomedical Technologies XV*, 1195103.

Bickler, P.E., Feiner, J.R & Severinghaus, J.W., (2005). Effects of Skin Pigmentation on Pulse Oximeter Accuracy at Low Saturation, *Anesthesiology*, 102: 715–9.

Bolic M. (2023). Pervasive Cardiovascular and Respiratory Monitoring Devices: Model-Based Design. Elsevier.

Cajas, S. A., Landínez, M. A. & López, D. M. (2020) Modeling of motion artifacts on PPG signals for heart-monitoring using wearable devices. *15th International Symposium on Medical Information Processing and Analysis,* 11330(3).

Chatterjee, S. & Phillips, J. P. (2017). Investigating optical path in reflectance pulse oximetry using a multilayer Monte Carlo model. *Clinical and Preclinical Optical Diagnostics*, edited by J. Quincy Brown, Ton G. van Leeuwen, Proc. of SPIE-OSA, 10411.

Fuentes-Guajardo, M., Latorre, K., León, D. & Martín-Escudero, P. (2022). Skin Pigmentation Influence on Pulse Oximetry Accuracy: A Systematic Review and Bibliometric Analysis. *Sensors*, 22(3402).

Hartmann, V., Liu, H., Chen, F., Qiu, Q., Hughes, S. & Zheng D. (2019). Quantitative Comparison of Photoplethysmographic Waveform Characteristics: Effect of Measurement Site. *Front Physiol.,* 10(198).

Mannheimer, P.D., et al. (2004). The Influence of Larger Subcutaneous Blood Vessels on Pulse Oximetry. Journal of Clinical Monitoring. 18, 179-88.

Marti, D., Aasbjerg, R. N., Andersen P. E. & Hansen A. K. (2018). MCmatlab: an open-source, user-friendly, MATLAB-integrated three-dimensional Monte Carlo light transport solver with heat diffusion and tissue damage. *Journal of Biomedical Optics*, SPIE, 23, 1-6..

Reuss, J. L., Siker, D. (2004). The pulse in reflectance pulse oximetry: Modeling and experimental studies. *Journal of Clinical Monitoring and Computing*, 18, 289–299.

Reuss, J.L. (2005). Multilayer modeling of reflectance pulse oximetry. *IEEE Trans Biomed Eng.*, 52(2), 153-159.

Teng, X.F. & Zhang, Y.T. (2004). The effect of contacting force on photoplethysmographic signals. Physiological Measurement, 25(5), 1323-1335.

Tuchin, V.V. (1997). Light scattering study in tissues. Physics—Uspekhhi, 40(5), 495–515.

Webster J. G. (Ed.) (1997). Design of Pulse Oximeters. IOP Publishing Ltd.

Wilson, B.C. & Adam, G. (1983). A Monte Carlo model for the absorption and flux distributions of light in tissue. *Med. Phys.*, 10(6), 824 – 830.

Zhou, C.C., Wang, J.Y., Qin, L.P. & Ye, X.S. (2020) Model Design and System Implementation for the Study of Anti-motion Artifacts Detection in Pulse Wave Monitoring. *Proceedings of the 13th International Joint Conference on Biomedical Engineering Systems and Technologies*, 1, 102-109.